

Intra- site $4f - 5d$ electronic correlations in the quadrupolar model of the $\gamma - \alpha$ phase transition in Ce.

A.V. Nikolaev^{1,2} and K.H. Michel¹

¹*Department of Physics, University of Antwerp, UIA, 2610 Antwerpen, Belgium*

²*Institute of Physical Chemistry of RAS, Leninskii prospect 31, 117915, Moscow, Russia*

As a possible mechanism of the $\gamma - \alpha$ phase transition in pristine cerium a change of the electronic density from a disordered state with symmetry $Fm\bar{3}m$ to an ordered state $Pa\bar{3}$ has been proposed. Here we include on-site and inter- site electron correlations involving one localized $4f$ -electron and one conduction $5d$ -electron per atom. The model is used to calculate the crystal field of γ -Ce and the temperature evolution of the mean-field of α -Ce. The formalism can be applied to crystals where quadrupolar ordering involves several electrons on the same site.

I. INTRODUCTION

Elemental solid cerium is known to undergo structural phase transitions.^{1,2} In the pressure-temperature phase diagram of Ce the puzzling long-standing problem is to understand the apparently isostructural transition between the cubic γ and α phases.^{1,3} An isostructural phase transformation can not be ascribed to a condensation of an order parameter and therefore can not be explained by the Landau theory of phase transitions. In the past, several models and theories have been suggested to address this problem.⁴⁻¹² Among them, a Mott like transition for $4f$ electrons^{4,5} and a Kondo effect based approach⁹⁻¹² are the competing ones. Also, new computational schemes have been applied to the problem using dynamical mean-field theory combined with the local density approximation.¹³

Under pressure above 5 GPa α -Ce becomes unstable and transforms first to a crystal with $C2/m$ or α -U space symmetry² (α' -Ce) and then to a body-centered tetragonal (bct) structure (α'' -Ce) above 12 GPa.¹⁴ This series of transformations can not be explained by invoking the concepts of the $4f$ localization-delocalization transition or Kondo volume collapse models and indicates that there are anisotropic interactions present in the α phase of cerium. Such electron interactions can be of quadrupolar origin that are known to drive symmetry lowering phase transitions in many lanthanide and actinide compounds.¹⁵

Recently, the isostructural character of the $\gamma - \alpha$ phase transition has been questioned by Eliashberg and Capellmann.¹⁶ They suggest that α -Ce should have a distorted fcc structure. Independently, the present authors have put forward a theory of quadrupolar ordering in cerium.^{17,18} There, it was proposed that the $\gamma - \alpha$ transformation is not really isostructural. Rather, it was associated with hidden electronic degrees of freedom.¹⁹ In our previous work, Refs. 17,18, we have suggested that the symmetry change is from $Fm\bar{3}m$ to $Pa\bar{3}$. This symmetry lowering is a special one. Although accompanied by a lattice contraction, it conserves the fcc structure of

the atomic center of mass points (cerium nuclei) and is solely due to orientational order of electronic densities. Such a scenario reconciles the $\gamma - \alpha$ transformation with the Landau theory of phase transitions. Our considerations for cerium have been inspired by the theory²⁰ of orientational phase transition in solid C_{60} where a similar space symmetry change ($Fm\bar{3}m \rightarrow Pa\bar{3}$) occurs at 255 K at room pressure.²¹

The present article is a continuation of our approach to the problem of the $\gamma - \alpha$ transition in Ce based on the technique of multipolar interactions between electronic densities of conduction and localized electrons in a crystal.^{17,18} Our second motivation is to extend our initial method, Ref. 17, for the case when two electrons (f - and d -) are at the same site of cerium and all intra- site interactions (including the on-site exchange) between them are taken into account. Our treatment of intra- site correlations is closely related with the method used by Condon and Shortley for many electron states of atoms.²² Provided that the average number of electrons per site is conserved this method is exact for intra- site correlations and goes beyond the usual self-consistent-field approach²³⁻²⁵ employed by band structure calculations.

Besides the problem of the $\gamma - \alpha$ phase transition in Ce, the microscopic method can be applied further²⁶ to describe quadrupolar ordering and to perform crystal field calculations of many f electrons on the same site. There are numerous compounds exhibiting quadrupolar ordering at low temperatures¹⁵ and there is a sustained interest in understanding their properties. Thus, recently DyB_2C_2 ,²⁷ DyB_6 ,²⁸ UCu_2Sn ,²⁹ $PrPb_3$,³⁰ $YbAs$,³¹ $YbSb$ ³² were reported to undergo a quadrupolar ordering.

II. THE MODEL

As follows from electronic band structure calculations of γ -Ce there exist three conduction electrons per atom which form the $(6s6p5d)^3$ metallic band and one local-

ized $4f$ electron.^{33,6–8} In our previous work, Ref. 18, we have already considered electric multipole interactions between conduction electrons and the localized $4f$ electrons. Below we focus on the on-site and inter-site correlations in the system and will simplify the model. We consider the instantaneous configuration $6s^25d4f$ as having the largest statistical weight on a cerium site (in comparison with other possibilities such as $6s6p5d4f$, $6s^25d^2$, $6s^24f^2$ and etc.). The two $6s$ electrons give only a spherically symmetrical density on the cerium site and their lowest energy state corresponds to a singlet. Therefore, as a first approximation we discard them as giving a closed shell. (Indeed, the level structure of $6s^25d4f$ corresponding to atomic Ce I is similar to that of $5d4f$ of La II³⁴) In fact, in doing so we omit the $s-d$ electron transitions which can contribute to the quadrupolar density.¹⁸ We are left then with one $5d$ conduction electron and one localized $4f$ electron. In the electronic band structure calculations the charge density of the $5d$ electron on the cerium site is considered as an average over all occupied \vec{k} states ($E(\vec{k}, \alpha) \leq E_F$, where α is the band index and E_F is the Fermi level). We have shown in Appendix B of Ref. 17 that the electron density is mainly spherical which corresponds to the standard “muffin-tin” (MT) treatment in electronic band structure calculations. The spherical density of $5d$ and $4f$ electrons will be the starting point in this work. We consider the $5d$ electron on a cerium center being instantaneously coupled with the $4f$ electron and include in the model all corresponding intra-site interactions, crystal electric field effects and inter-site multipolar electric interactions. From the technical point of view, this fd -model is a many electron generalization of the concepts of Ref. 17. We are aware that the model based on the fd -configuration is incomplete, but it has an advantage of taking into account all intra-site interactions (often referred to as Hund’s rules) which are usually omitted in the electron band structure calculations.^{23,24} Later we will briefly discuss a possibility to refine our model with the help of the valence bond (or Heitler-London) theory of chemical bonding.^{35,36}

We consider a face centered cubic (fcc) crystal of N Ce atoms. Each atomic site possesses one $4f$ and one $5d$ electron. The position vector of an electron near a crystal lattice site \vec{n} is given by

$$\vec{R}(\vec{n}) = \vec{X}(\vec{n}) + \vec{r}(\vec{n}). \quad (2.1)$$

Here $\vec{X}(\vec{n})$ is the lattice vector which specifies the centers of the atoms (or Ce-nuclei) on a rigid fcc lattice. The radius vector $\vec{r}(\vec{n})$ is given in polar coordinates by $(r(\vec{n}), \Omega(\vec{n}))$, where r is the length and $\Omega = (\Theta, \phi)$ stands for the polar angles. We label the two-electron basis ket-vectors at a lattice site \vec{n} by a single index I_{fd} or, alternatively, by the pair of single electron indices (i_f, i_d) :

$$|I_{fd}\rangle_{\vec{n}} = |i_f; i_d\rangle_{\vec{n}}. \quad (2.2)$$

The index i stands for the electron orbital and spin projection quantum numbers. The corresponding basis wave

functions are

$$\langle \vec{r}, \vec{r}' | I_{fd} \rangle_{\vec{n}} = \langle \vec{r} | i_f \rangle_{\vec{n}} \cdot \langle \vec{r}' | i_d \rangle_{\vec{n}}, \quad (2.3)$$

where

$$\langle \vec{r} | i_f \rangle_{\vec{n}} = \mathcal{R}_f(r(\vec{n})) \langle \hat{n} | i_f \rangle, \quad (2.4a)$$

$$\langle \vec{r}' | i_d \rangle_{\vec{n}} = \mathcal{R}_d(r'(\vec{n})) \langle \hat{n}' | i_d \rangle. \quad (2.4b)$$

Here \mathcal{R}_f and \mathcal{R}_d are radial components of the $4f$ and the $5d$ electron, respectively; \hat{n} stands for $\Omega(\vec{n})$. There are 14 orientational vectors (or spin-orbitals) $\langle \hat{n} | i_f \rangle$ for a $4f$ electron ($i_f=1-14$) and 10 orientational vectors $\langle \hat{n}' | i_d \rangle$ for a $5d$ electron ($i_d=1-10$). These spin-orbitals can be written as

$$\langle \hat{n} | i_f \rangle = \langle \hat{n} | m_f \rangle u_s(s_z(f)), \quad (2.5a)$$

$$\langle \hat{n}' | i_d \rangle = \langle \hat{n}' | m_d \rangle u_s(s_z(d)). \quad (2.5b)$$

Here u_s is the spin function ($s = \pm$) for the spin projections $s_z = \pm 1/2$ on the z -axis. The orbital parts, $\langle \hat{n} | m_f \rangle$ ($m_f=1-7$) and $\langle \hat{n}' | m_d \rangle$ ($m_d=1-5$), are expressed in terms of spherical harmonics $Y_l^m(\Omega) = \langle \hat{n} | l, m \rangle$. We find it convenient to work with real spherical harmonics. We consider

$$\{Y_3^0, Y_3^{1c}, Y_3^{1s}, Y_3^{2c}, Y_3^{2s}, Y_3^{3c}, Y_3^{3s}\} = \langle \hat{n} | m_f \rangle \quad (2.6a)$$

for $4f$ electron (corresponding to $m_f = 1 - 7$) and

$$\{Y_2^0, Y_2^{1c}, Y_2^{1s}, Y_2^{2c}, Y_2^{2s}\} = \langle \hat{n}' | m_d \rangle \quad (2.6b)$$

for $5d$ electron (corresponding to $m_d = 1 - 5$). We use the definition of real spherical harmonics of Ref. 37 (see also explicit expressions (2.1) in Ref. 17) that is different from the definition of Condon and Shortley.²² The advantage of using the basis with real spherical harmonics is that the matrix elements of Coulomb and exchange interactions stay real.

The order of indices in (2.2) and (2.3) is important if we associate the first electron with the f state i_f while the second with the d state i_d . Then in addition to the vectors (2.2) we have to consider the states described by the vectors $|i_d; i_f\rangle_{\vec{n}}$ (the first electron is in the i_d state and the second is in the i_f state). However, from the dynamical equivalence of the electrons we can permute the spin-orbitals to the standard order, Eq. (2.2), by using

$$|i_d; i_f\rangle_{\vec{n}} = -|i_f; i_d\rangle_{\vec{n}}, \quad (2.7)$$

since it requires the interchange of the two electrons. In order to describe the same quantum state $(i_f; i_d)$ we will use the basis vectors (2.2) and apply (2.7) when needed. (Alternatively, one can use the procedure of antisymmetrization of the basis vectors (2.2) as described elsewhere.) Thus, our basis (2.2) consists of 140 different vectors $|I_{fd}\rangle$.

The ground state energy of the $(4f5d)$ electron system, E_0 , can be calculated in local density approximation (LDA) with spherically symmetric Coulomb and exchange potentials. Going beyond this model in atomic

cerium, one has to take into account multipolar on-site (also called intra- site) Coulomb interactions and spin-orbit coupling. In solid cerium, the interactions with conduction electrons and inter- site Coulomb interactions still have to be added.

In the following we will study these effects within a unified formalism based on a multipole expansion of the Coulomb potential and of the systematic use of site symmetry of the crystal lattice. For the case of on-site Coulomb interactions between two electrons (charge $e = -1$) we have

$$V(\vec{R}(\vec{n}), \vec{R}'(\vec{n}')) = \frac{1}{|\vec{r}(\vec{n}) - \vec{r}'(\vec{n}')|}. \quad (2.8)$$

The multipole expansion in terms of site symmetry adapted functions (SAF's) $S_\Lambda(\hat{n})$ reads:

$$V(\vec{R}(\vec{n}), \vec{R}'(\vec{n}')) = \sum_{\Lambda} v_{\Lambda\Lambda'}(r, r') S_\Lambda(\hat{n}) S_{\Lambda'}(\hat{n}'), \quad (2.9a)$$

where

$$v_{\Lambda\Lambda'}(r, r') = \left(\frac{r_{<}^l}{r_{>}^{(l+1)}} \right) \frac{4\pi}{2l+1} \delta_{\Lambda\Lambda'}, \quad (2.9b)$$

with $r_{>} = \max(r, r')$, $r_{<} = \min(r, r')$ and $\delta_{\Lambda\Lambda'} = \delta_{\tau\tau'} \delta_{\mu\mu'}$. Clearly, the last expression is site independent. The SAF's are linear combinations of spherical harmonics and transform as irreducible representations of the site point group, Ref. 37. The index Λ stands for (l, τ) , with $\tau = (\Gamma, \mu, k)$. Here l accounts for the angular dependence of the multipolar expansion, Γ denotes an irreducible representation (in the present case of the group O_h), μ labels the representations that occur more than once and k denotes the rows of a given representation.

On the other hand, the Coulomb interaction between two electrons at different sites $\vec{n} \neq \vec{n}'$ (inter- site) reads

$$V(\vec{R}(\vec{n}), \vec{R}'(\vec{n}')) = \frac{1}{|\vec{R}(\vec{n}) - \vec{R}'(\vec{n}')|}. \quad (2.10)$$

The multipole expansion is given by

$$V(\vec{R}(\vec{n}), \vec{R}'(\vec{n}')) = \sum_{\Lambda\Lambda'} v_{\Lambda\Lambda'}(\vec{n}, \vec{n}'; r, r') S_\Lambda(\hat{n}) S_{\Lambda'}(\hat{n}'), \quad (2.11a)$$

where

$$v_{\Lambda\Lambda'}(\vec{n}, \vec{n}'; r, r') = \int d\Omega(\vec{n}) \int d\Omega'(\vec{n}') \frac{S_\Lambda(\hat{n}) S_{\Lambda'}(\hat{n}')}{|\vec{R}(\vec{n}) - \vec{R}'(\vec{n}')|}. \quad (2.11b)$$

The inter- site multipole expansion (2.11a) is anisotropic and converges fast since³⁸

$$v_{\Lambda\Lambda'}(\vec{n}, \vec{n}'; r, r') \sim \frac{(r)^l (r')^{l'}}{|\vec{X}(\vec{n}) - \vec{X}'(\vec{n}')|^{l+l'+1}}. \quad (2.12)$$

Therefore, it is sufficient to consider it only for nearest neighbors. From the practical point of view, one can calculate $v_{\Lambda\Lambda'}(\vec{n}, \vec{n}'; r_0, r'_0)$ only for two fixed radii r_0 and r'_0 . Then one obtains $v_{\Lambda\Lambda'}(\vec{n}, \vec{n}'; r, r')$ as a function of r and r' by employing the dependence (2.12).

III. THE INTRA- SITE INTERACTIONS

The interactions which we analyze in this section are present already in atomic cerium.^{22,34} We have considered a part of these correlations in previous work,¹⁸ and here we study all of them in the framework of the fd -model. In fact, these multipole interactions are responsible for the electronic terms of atoms.²² We will see that their combined effect lowers the energy of the cerium atom by $\sim 1 - 2$ eV in comparison with the spherically symmetric case, yet usually they are not taken into account in the electronic band structure calculations in solids. Although our consideration in this section is based on the original technique for multipole interactions,¹⁷ it overlaps largely with the method of Condon and Shortley.²² However, for two reasons we have decided to briefly review it here. Firstly, we consider below a more general case which is not limited by the LS (Russell-Saunders) coupling and the consideration of diagonal matrix elements. Secondly, the results of this section are used to describe crystal electric field effects and the phase transition to the $Pa\bar{3}$ structure.

The direct matrix elements for the intra- site Coulomb interactions are obtained if we consider only the $f - f$ transitions for the first electron and the $d - d$ transitions for the second. We start from Eq. (2.9a) and obtain

$$\begin{aligned} & \langle I_{fd} | \bar{n} V(\vec{R}(\vec{n}), \vec{R}'(\vec{n}')) | J_{fd} \rangle_{\bar{n}}^{Coul} \\ &= \sum_{\Lambda} v_{\Lambda\Lambda}^{FD} c_\Lambda(i_f j_f) c_\Lambda(i_d j_d), \end{aligned} \quad (3.1)$$

where

$$v_{\Lambda\Lambda}^{FD} = \int dr r^2 \int dr' r'^2 \mathcal{R}_f^2(r) \mathcal{R}_d^2(r') v_{\Lambda\Lambda}(r, r') \quad (3.2)$$

accounts for the average radial dependence while $v_{\Lambda\Lambda}(r, r')$ is given by Eq. (2.9b). We use the superscripts F and D in order to indicate that we have transitions between two $4f$ states ($F \equiv (f, f)$) and the transitions between two $5d$ states ($D \equiv (d, d)$). The elements c_Λ are defined by

$$c_\Lambda(i_f j_f) = \int d\Omega \langle i_f | \hat{n} \rangle S_\Lambda(\hat{n}) \langle \hat{n} | j_f \rangle, \quad (3.3a)$$

$$c_\Lambda(i_d j_d) = \int d\Omega \langle i_d | \hat{n} \rangle S_\Lambda(\hat{n}) \langle \hat{n} | j_d \rangle. \quad (3.3b)$$

The other possibility is to consider the transitions $4f \rightarrow 5d$ for the first electron and the transitions $5d \rightarrow 4f$

for the second. This gives the exchange interactions and then we should use (2.7) in order to return to the standard order of the spin-orbitals. We find

$$\begin{aligned} & \langle I_{fd} | \bar{n} V(\bar{R}(\bar{n}), \bar{R}'(\bar{n})) | J_{fd} \rangle_{\bar{n}}^{exch} \\ &= - \sum_{\Lambda} v_{\Lambda\Lambda}^{(fd)(df)} c_{\Lambda}(i_f j_d) c_{\Lambda}(i_d j_f), \end{aligned} \quad (3.4)$$

where

$$\begin{aligned} v_{\Lambda}^{(fd)(df)} &= \int dr r^2 \int dr' r'^2 \mathcal{R}_f(r) \mathcal{R}_d(r) \mathcal{R}_d(r') \mathcal{R}_f(r') \\ & \times v_{\Lambda\Lambda}(r, r'), \end{aligned} \quad (3.5)$$

and

$$c_{\Lambda}(i_f j_d) = \int d\Omega \langle i_f | \hat{n} \rangle S_{\Lambda}(\hat{n}) \langle \hat{n} | j_d \rangle, \quad (3.6a)$$

$$c_{\Lambda}^{df}(i_d j_f) = \int d\Omega \langle i_d | \hat{n} \rangle S_{\Lambda}(\hat{n}) \langle \hat{n} | j_f \rangle. \quad (3.6b)$$

We observe that in the basis with real orbitals, Eq. (2.6a,b), and with real functions S_{Λ} the coefficients c_{Λ} are real and we get

$$c_{\Lambda}(i_d j_f) = c_{\Lambda}(j_f i_d). \quad (3.7)$$

We start with the description of spherically symmetric terms ($l = 0$) corresponding to the trivial function $S_0 = 1/\sqrt{4\pi}$. The coefficients c_{Λ} in (3.3a,b) become diagonal,

$$c_{l=0}(i_d j_d) = \frac{1}{\sqrt{4\pi}} \delta_{i_d j_d}, \quad c_{l=0}(i_f j_f) = \frac{1}{\sqrt{4\pi}} \delta_{i_f j_f}, \quad (3.8)$$

while $c_{l=0}(i_f j_d) = c_{l=0}(i_d j_f) = 0$. Hence, we obtain a contribution to $\langle I | V | J \rangle^{Coul}$ which is proportional to the unit matrix. Since it corresponds only to a shift of the ground state energy, it is irrelevant.

In considering the other contributions (with $l > 0$) in (3.1) and (3.4) we will take advantage of the selection rules imposed by the coefficients c_{Λ} , Eqs. (3.3a,b) and (3.6a,b). First of all, we notice that the coefficients c_{Λ} are diagonal in terms of spin components u_s . From the theory of addition of angular momenta (see, for example, Ref. 36) we know that nonzero coefficients $c_{\Lambda}(i_f j_f)$ can occur if l (in Λ) equals to 0,1,2,...,6, Eq. (3.3a). Furthermore, the odd values of l are excluded due to the parity of the integrand in (3.3a) and finally we obtain that $l = 0, 2, 4$ and 6 . Analogously, for the $d-d$ transitions the allowed coefficients are with $l = 0, 2$ and 4 , Eq. (3.3b). For the $f-d$ transitions, Eq. (3.6a,b) we find that $l = 1, 3$ and 5 . Next we notice that if the radial parts, \mathcal{R}_f , \mathcal{R}_d , are the same for all spin-orbitals of $4f$ and $5d$ states, correspondingly, then the integrals (3.2) and (3.5) depend only on l . We can condense the notation, $v_l^{FD} = v_{\Lambda\Lambda}^{FD}$ for $l = 0, 2$ and 4 ; and $v_l^{(fd)} = v_{\Lambda}^{(fd)(df)}$ for $l' = 1, 3$ and 5 . In fact, these integrals are proportional to F^k and G^k in the notations of Condon and Shortley,²²

$$\begin{aligned} v_2^{FD} &= \frac{4\pi}{5} F^2(4f, 5d), & v_4^{FD} &= \frac{4\pi}{9} F^4(4f, 5d) \\ v_1^{(fd)} &= \frac{4\pi}{3} G^1(4f, 5d), & v_3^{(fd)} &= \frac{4\pi}{7} G^3(4f, 5d), \\ v_5^{(fd)} &= \frac{4\pi}{11} G^5(4f, 5d). \end{aligned} \quad (3.9)$$

(Notice however that our coefficients c_{Λ} are different from those of Condon and Shortley.²²) We have estimated the integrals in (3.9) from the radial dependences \mathcal{R}_f and \mathcal{R}_d obtained from calculations on a cerium atom in local density approximation (LDA). We have found that $v_2^{FD} = 85858$, $v_4^{FD} = 24260$, $v_1^{(fd)} = 83128$, $v_3^{(fd)} = 26563$ and $v_5^{(fd)} = 12584$, in K (Kelvin).

Finally, we rewrite expressions (3.1) and (3.4) in matrix form as

$$\begin{aligned} & \langle I_{fd} | V(intra) | J_{fd} \rangle^{Coul} = \\ & v_2^{FD} c_2^{FD}(I_{fd} | J_{fd}) + v_4^{FD} c_4^{FD}(I_{fd} | J_{fd}), \end{aligned} \quad (3.10a)$$

and

$$\begin{aligned} & \langle I_{fd} | V(intra) | J_{fd} \rangle^{exch} = -[v_1^{(fd)} c_1^{(fd)}(I_{fd} | J_{fd}) \\ & + v_3^{(fd)} c_3^{(fd)}(I_{fd} | J_{fd}) + v_5^{(fd)} c_5^{(fd)}(I_{fd} | J_{fd})], \end{aligned} \quad (3.10b)$$

Here the direct Coulomb matrices $c_l^{FD}(I_{fd} | J_{fd})$ are defined as

$$c_l^{FD}(I_{fd} | J_{fd}) = \left(\sum_{\tau} c_{(l,\tau)}(i_f j_f) c_{(l,\tau)}(i_d j_d) \right), \quad (3.11a)$$

where $l = 2$ and 4 ; and the three ‘‘exchange’’ matrices $c_l^{(fd)}(I_{fd} | J_{fd})$ ($l = 1, 3$ and 5) are given by

$$c_l^{(fd)}(I_{fd} | J_{fd}) = \left(\sum_{\tau} c_{(l,\tau)}(i_f j_d) c_{(l,\tau)}(i_d j_f) \right). \quad (3.11b)$$

We solve the secular problem for the 140×140 matrix of intra- site interactions

$$\begin{aligned} & \langle I_{fd} | V(intra) | J_{fd} \rangle = \\ & \langle I_{fd} | V(intra) | J_{fd} \rangle^{Coul} + \langle I_{fd} | V(intra) | J_{fd} \rangle^{exch}, \end{aligned} \quad (3.12)$$

and obtain the ten energy levels E_{fd} quoted in column 2 and 3 of Table I. This term spectrum corresponds to the usual LS (Russell-Saunders) coupling without spin-orbit interactions. We have also checked our results by working with the eigenvectors of (3.12) which can be obtained independently by exploiting the formulas (Table 4³ of Ref. 22) of vector addition of angular momenta ($j_1 = 3$ and $j_2 = 2$). The levels of Table I correspond to the following parameters in the notations of Condon and Shortley,²² $F_2 = 325.4$, $F_4 = 25.1$, $G_1 = 567$, $G_3 = 47$ and $G_5 = 7.2$ (in K) (These parameters should not be confused with those in (3.9)).

We now consider the effect of the spin-orbit coupling. Starting with the spherically symmetric LDA calculation

TABLE I. Term energies of the fd configuration in the absence of spin-orbit coupling, E_m and ΔE stand for the singlet-triplet energy means and the singlet-triplet energy differences, respectively. L is the orbital quantum number of the two electrons. The energy corresponding to the spherically symmetric description is taken as zero. All energies are in units K.

L	singlets	triplets	E_m	ΔE
P	13541.8	5384.5	9463.1	8157.3
D	-3011.8	1951.8	-530.0	-4963.5
F	2767.8	-6616.1	-1924.1	9383.9
G	-9378.4	-1485.3	-5431.8	-7893.1
H	12310.8	-5653.4	3328.7	17964.2

of a cerium atom we obtain that in the one-electron approximation $\Delta_{so}(f) = E_f(7/2) - E_f(5/2) = 4003.4$ K and $\Delta_{so}(d) = E_d(5/2) - E_d(3/2) = 2344.0$ K. This gives for the spin-orbit coupling constants $\zeta_f = 1143.8$ K and $\zeta_d = 937.6$ K. Therefore, a typical value of spin-orbit splitting is ~ 1000 K which shows that it can not be treated as a small perturbation to the LS term scheme, Table I. In order to take into account the spin-orbit coupling exactly we have to consider the operator

$$V_{so} = V_{so}(f) + V_{so}(d), \quad (3.13)$$

where

$$V_{so}(f) = \zeta_f \vec{L}(f) \cdot \vec{S}(f), \quad (3.14a)$$

$$V_{so}(d) = \zeta_d \vec{L}(d) \cdot \vec{S}(d). \quad (3.14b)$$

The matrix of interactions reads

$$\langle I_{fd} | V_{so} | J_{fd} \rangle = (\langle i_f | V_{so}(f) | j_f \rangle \delta_{i_d j_d} + \langle i_d | V_{so}(d) | j_d \rangle \delta_{i_f j_f}). \quad (3.15)$$

Since we know the matrix elements $\langle i_f | V_{so}(f) | j_f \rangle$ and $\langle i_d | V_{so}(d) | j_d \rangle$ (see for example the explicit Eq. (A.2) of Ref. 17) we can calculate the matrix elements for the fd -configuration. We now solve the secular problem for the sum of the intra-site and spin-orbit interactions, starting from the matrix of

$$U|_{intra} = V(intra) + V_{so}, \quad (3.16)$$

and obtain 20 energy levels $\{E_{fd}\}$. Since we are interested only in the lowest levels, we quote in Table II the first six out of the 20 levels. (The procedure of calculation of magnetic moments and the Lande g -factors is given in Appendix A.)

Comparison with the experimental data³⁴ on a Ce atom shows that the order of the three lowest levels, 1G_4 , 3F_2 and 3H_4 , with the multiplet 1G_4 as the ground state is correct. On the other hand, the experimental data show that in atomic Ce different levels (such as 1G , 3F , 3H) are considerably mixed up. Due to the strong spin-orbit coupling there is an appreciable mixing between

TABLE II. Calculated lowest term energies of the fd configuration with the spin-orbit coupling and the Lande g -factors (columns 2-4), $\Delta E = E_{fd} - E_{fd}(^1G_4)$. Last two columns are experimental data, Ref. 34. All energies are in units K.

	E_{fd}	g	ΔE	Ce I	La II (fd)
1G_4	-10570.3	0.9323	0	0	0
3F_2	-9226.5	0.7030	1343.8	329.2	881.7
3H_4	-8155.1	0.8958	2415.2	1840.9	1764.7
3F_3	-7048.8	1.0825	3521.5	2393.0	2354.5
3H_5	-6449.4	1.0334	4120.9	3177.9	2850.7
3G_3	-4247.3	0.7659	6323.0	1998.5	5472.8

1G_4 and 3H_4 , and between 3F_2 and 1D_2 . The ground state of a Ce atom has 55% of 1G_4 and 29% of 3H_4 .³⁴ The next level which lies only 329 K above the ground state has 66% of 3F_2 and 24% of 1D_2 .³⁴ In conclusion, although the actual atomic spectra of cerium differ somewhat from our results obtained for the fd -configuration, Table II, our approach captures the main properties and we will use it for Ce in the solid state. In the following we will extend the calculations of the energy level scheme by including inter-site interactions. We will treat separately the γ and the α phase of solid Ce.

IV. INTER- SITE INTERACTIONS

In this section we will first consider the matrix of inter-site interactions for the (fd) system on a crystal in general. Next we will show that the interaction is largely simplified by crystal symmetry and derive the crystal electric field (CEF). We calculate the energy spectrum of the (fd) system in presence of the crystal electric field in the disordered cubic phase.

We start from expression (2.11a) and write it in the space of two electron state vectors $|I_{fd}\rangle$. Carrying out the angular integrations $d\Omega(\vec{n})$, $d\Omega'(\vec{n})$, $d\Omega(\vec{n}')$, $d\Omega'(\vec{n}')$, we obtain

$$\begin{aligned} & \langle I_{fd} | \vec{n} \langle I'_{fd} | \vec{n}' V(\vec{R}(\vec{n}), \vec{R}'(\vec{n}')) | J'_{fd} \rangle \vec{n}' | J_{fd} \rangle \vec{n} = \\ & \sum_{\alpha\beta} \sum_{\alpha'\beta'} \sum_{\Lambda\Lambda'} v_{\Lambda}^{\alpha\alpha'} v_{\Lambda'}^{\alpha'\alpha'} (\vec{n} - \vec{n}') \\ & \times \{c_{\Lambda}(i_{\alpha}j_{\alpha}) \delta(i_{\beta}j_{\beta})\} \{c_{\Lambda'}(i_{\alpha'}j_{\alpha'}) \delta(i_{\beta'}j_{\beta'})\}, \quad (4.1) \end{aligned}$$

Here each of the indices α , α' , β , β' runs over the labels f , d . The coefficients c_{Λ} are defined by Eqs. (3.6a) and (3.6b), while $\delta(i_{\beta}j_{\beta})$ stands for the Kronecker delta symbol. For $\alpha = f$, we have $\beta = d$ and for $\alpha = d$, $\beta = f$, with a similar correspondence between α' and β' . The inter-site interaction element $v_{\Lambda}^{\alpha\alpha'} v_{\Lambda'}^{\alpha'\alpha'}$ is given by

$$\begin{aligned} v_{\Lambda}^{\alpha\alpha'} v_{\Lambda'}^{\alpha'\alpha'} (\vec{n} - \vec{n}') &= \int dr r^2 \int dr' r'^2 \\ &\times \mathcal{R}_{\alpha}^2(r) \mathcal{R}_{\alpha'}^2(r') v_{\Lambda\Lambda'}(\vec{n}, \vec{n}'; r, r'), \quad (4.2) \end{aligned}$$

Notice that only direct Coulomb interactions are present in (4.1), and with the help of the selection rules for the coefficients c_Λ we conclude that only the interactions with $l = 0, 2, 4$ and 6 have to be considered.

A. The crystal electric field (γ -phase)

In the γ -phase the electronic density is compatible with the crystal structure $Fm\bar{3}m$. At each atomic site the crystal electric field (CEF) has the point group symmetry O_h . In lowest approximation, the CEF corresponds to the potential experienced by a charge at a central site \vec{n} , when spherically symmetric ($l' = 0$) contributions from charge densities at the twelve neighboring sites \vec{n}' on the fcc lattice and similar terms from the electronic density in the interstitial regions are taken into account. Previously^{17,18} these effects were studied for a single $4f$ electron per Ce atom. Here we present an extension to the ($4f5d$) system.

In crystal field approximation the functions $S_{\Lambda'}(\vec{n}')$ at any of the twelve sites \vec{n}' reduce to $Y_0^0 = 1/\sqrt{4\pi}$. We will write an index 0 for Λ' ($l' = 0, A_{1g}$). The coefficients $c_{\Lambda'}$ in Eq. (4.1) now reduce to

$$c_0(i_{\alpha'} j_{\alpha'}) = \frac{1}{\sqrt{4\pi}} \delta(i_{\alpha'}, j_{\alpha'}). \quad (4.3)$$

At the central site \vec{n} , the electronic density has full cubic symmetry. We denote the corresponding SAF's by $S_{\Lambda_1}(\vec{n})$, $\Lambda_1 \equiv (l, A_{1g})$, where A_{1g} stands for the unit representation of the cubic site group O_h . We retain the functions for $l = 4$ and $l = 6$, which correspond to the cubic harmonics K_4 and K_6 . The selection rules imply that the $d-d$ transitions are perturbed by K_4 only, while for the $f-f$ transitions both K_4 and K_6 are relevant. Expression (2.11a) reduces to

$$V(\vec{R}(\vec{n}), \vec{R}'(\vec{n}')) = \frac{1}{\sqrt{4\pi}} \sum_{\Lambda_1} v_{\Lambda_1 0}(\vec{n}, \vec{n}'; r, r') S_{\Lambda_1}(\vec{n}). \quad (4.4a)$$

The elements

$$v_{\Lambda_1 0}(\vec{n}, \vec{n}'; r, r') = \frac{1}{\sqrt{4\pi}} \int d\Omega(\vec{n}) \int d\Omega'(\vec{n}') \frac{S_{\Lambda_1}(\hat{n})}{|\vec{R}(\vec{n}) - \vec{R}'(\vec{n}')|} \quad (4.4b)$$

have the same value for all twelve neighbors \vec{n}' on the fcc lattice. In addition they are independent of r' , as follows from expression (2.12) for $l' = 0$. We then define the crystal field operator by

$$V_{CF}(\vec{R}(\vec{n})) = \frac{12}{\sqrt{4\pi}} \sum_{\Lambda_1} v_{\Lambda_1 0}(\vec{n}, \vec{n}'; r, r') S_{\Lambda_1}(\vec{n}). \quad (4.5)$$

Returning to expression (4.2) we write within the crystal field approximation

$$v_{\Lambda_1 0}^{\alpha\alpha'}(\vec{n} - \vec{n}') = v_{\Lambda_1 0}^{\alpha\alpha\bullet} \cdot Q_{\alpha'}, \quad (4.6a)$$

where

$$v_{\Lambda_1 0}^{\alpha\alpha\bullet} = \int dr r^2 \mathcal{R}_\alpha^2(r) v_{\Lambda_1 0}(\vec{n}, \vec{n}'; r, r') \quad (4.6b)$$

and

$$Q_{\alpha'} = \int dr' r'^2 \mathcal{R}_{\alpha'}^2(r'). \quad (4.6c)$$

Notice that $Q_{\alpha'}$ stands for Q_f or Q_d which are charges (in units e) of the $4f$ or $5d$ electron. As before^{17,18} the integration is taken over $0 < r' < R_{MT}$, where R_{MT} is the radius of the muffin-tin sphere. Besides $4f$ and $5d$ electrons we can also consider similar contributions from $6s$ electrons and nuclei belonging to nearest neighbors. Notice that the interaction parameters $v_{\Lambda_1 0}^{ff\bullet}$ and $v_{\Lambda_1 0}^{dd\bullet}$, Eq. (4.6b), remain the same for all these contributions and all we have to do is to collect the charges together. Finally, after summation over 12 nearest neighbors and simplifications, we obtain

$$\langle I_{fd} | \vec{n} V_{CF}(\vec{R}(\vec{n})) | J_{fd} \rangle_{\vec{n}} = \sum_{\Lambda_1} \left[B_{\Lambda_1}^f c_{\Lambda_1}(i_f j_f) \delta(i_d j_d) + B_{\Lambda_1}^d c_{\Lambda_1}(i_d j_d) \delta(i_f j_f) \right], \quad (4.7)$$

where

$$B_{\Lambda_1}^f = \frac{12}{\sqrt{4\pi}} Q_{eff} e v_{\Lambda_1 0}^{F\bullet}, \quad (4.8a)$$

$$B_{\Lambda_1}^d = \frac{12}{\sqrt{4\pi}} Q_{eff} e v_{\Lambda_1 0}^{D\bullet}. \quad (4.8b)$$

Here again we write D for (dd) and F for (ff). We take as an effective charge $Q_{eff} = Q_{MT}$, the total charge inside a MT-sphere. In contradistinction to our previous work^{17,18} here we have neglected the effect of interstitial charges. Previously it was found that a *homogeneous* distribution of negative charge in the interstices increases the effective charge by an amount $2.85Q_{MT}$. This fact due to the angular dependence of the leading cubic harmonic S_{Λ_1} , $\Lambda_1 = (l = 4, A_{1g})$ in Eq. (4.4b). Indeed $K_4(\hat{n})$ is positive and maximum along the cubic direction $[100]$ (the centers of the interstices) and negative and small along $[110]$ (the sites \vec{n}'). On the other hand, if we consider an inhomogeneous charge distribution where most of the electronic density in the interstices is located close to $[110]$, then the contribution to the crystal field from interstitial charges can be assumed to be negligibly small. We observe that previously the inclusion of contributions from a homogeneous charge distribution in the interstices has led to an overestimation of calculated crystal field splitting in comparison with the experimental values.¹⁸

In practice, it is convenient to calculate $v_{\Lambda_1 0}^{\alpha\alpha\bullet}$ from

$$v_{\Lambda_1 0}^{\alpha\alpha\bullet} = \frac{v_{\Lambda_1 0}(\vec{n}, \vec{n}'; R_{MT}, r')}{R_{MT}^l} q_l^\alpha, \quad (4.9a)$$

where

$$q_l^\alpha = \int dr' r'^{(l+2)} \mathcal{R}_\alpha^2(r'). \quad (4.9b)$$

Then the CEF operator (4.5), with an effective charge Q_{eff} , can be rewritten as

$$V_{CF}(\vec{R}(\vec{n})) = \sum_{\Lambda_1} B_{\Lambda_1} S_{\Lambda_1}(\hat{n}) r^l, \quad (4.10a)$$

where³⁹

$$B_{\Lambda_1} = \frac{12}{\sqrt{4\pi}} Q_{eff} e \frac{v_{\Lambda_1 0}(\vec{n}, \vec{n}'; R_{MT}, f')}{R_{MT}^l}. \quad (4.10b)$$

Our calculations for γ -Ce ($a=9.753$ a.u.) yield $Q_{MT} = +0.9136 |e|$,⁴⁰ $q_4^d/R_{MT}^4=0.22271$, $q_4^f/R_{MT}^4=0.03604$, $q_6^f/R_{MT}^6 = 0.01739$ (in a.u.), and $B_4^d=1198.4$, $B_4^f=193.9$, $B_6^f=74.4$ (all in K).⁴¹ We then consider the Hamiltonian

$$H^\gamma(\vec{n}) = U|_{intra} + V_{CF}(\vec{n}), \quad (4.11)$$

which we associate with the γ phase of Ce. By diagonalizing H^γ we have found that in the cubic CEF the twenty atomic-like levels of cerium are split into 58 distinct sub-levels which can be labeled by single valued irreducible representations $A_1(\Gamma_1)$, $E(\Gamma_3)$, $T_1(\Gamma_4)$ and $T_2(\Gamma_5)$ of O_h . In particular, three lowest levels of cerium are split according to the following scheme,^{42,36}

$${}^1G_4 \rightarrow A_1 + T_1 + E + T_2, \quad (4.12a)$$

$${}^3F_2 \rightarrow T_2 + E, \quad (4.12b)$$

$${}^3H_4 \rightarrow T_2 + A_1 + T_1 + E. \quad (4.12c)$$

The calculated splittings of these levels are quoted in Table III. In presence of a magnetic field, there occurs an additional splitting of the triplets. The corresponding magnetic moments are given in the last column of Table III. (Details of the calculations can be found in Appendix A.) In the second part of the present section we will study the energy levels in the ordered phase.

B. Quadrupolar ordering (α -phase)

In the cubic phase (γ -Ce) with the $Fm\bar{3}m$ space symmetry the nontrivial electron density distribution is given by cubic harmonics $K_4(\Omega)$ and $K_6(\Omega)$ with $l = 4$ and 6 . All quadrupole densities with $l = l' = 2$ average to zero. Only fluctuations of electric quadrupoles are allowed in the interaction Eq. (4.1) and those lead to an effective attractive interaction at the X point of the Brillouin zone.^{17,18} This interaction drives a transition to a new phase which is characterized by an ordering of electric quadrupoles such that the space group symmetry is $Pa\bar{3}$. This order-disorder transition is accompanied

TABLE III. Lowest levels of the energy spectrum of $H^\gamma = U|_{intra} + V_{CF}$, γ -Ce. Numbers in parentheses stand for degeneracy; $\Delta\varepsilon_1 = 1409.6$ K, $\Delta\varepsilon_2 = 2499.4$ K; the site group is O_h .

Γ, μ		ε_i , in K	$(\varepsilon_i - \varepsilon_1)$, in K	\mathcal{M}_z , in μ_B
$A_1, 1$	(1)	-10661.1	0.0	0
$T_1, 1$	(3)	-10613.7	47.4	± 0.4596 ; 0
$E, 1$	(2)	-10580.9	80.2	0; 0
$T_2, 1$	(3)	-10505.6	155.5	± 2.3112 ; 0
$T_2, 2$	(3)	-9251.5	$\Delta\varepsilon_1$	± 0.6634 ; 0
$E, 2$	(2)	-9224.4	$\Delta\varepsilon_1 + 27.1$	0; 0
$T_1, 2$	(3)	-8161.7	$\Delta\varepsilon_2$	± 2.2447 ; 0
$T_2, 3$	(3)	-8154.2	$\Delta\varepsilon_2 + 7.5$	± 0.4503 ; 0
$A_1, 2$	(1)	-8145.9	$\Delta\varepsilon_2 + 15.8$	0
$E, 3$	(2)	-8137.5	$\Delta\varepsilon_2 + 24.2$	0; 0

by a contraction of the crystal lattice which stays cubic. We have associated this phase transition with the $\gamma \rightarrow \alpha$ transition of Ce. In real space the $Pa\bar{3}$ ordering implies the appearance of four distinct sublattices of simple cubic structure (see Fig. 3 of Ref. 17). We label these sublattices which contain the sites $(0,0,0)$ $(a/2)(0,1,1)$, $(a/2)(1,0,1)$ and $(a/2)(1,1,0)$ by $\{\vec{n}_p\}$, $p = 1 - 4$, respectively. In principle, one can proceed as in Ref. 17 and derive an effective mean-field Hamiltonian. Here we will start from the crystal in real space and consider the following four quadrupolar SAF's corresponding to the four sublattices of $Pa\bar{3}$:

$$\mathcal{S}_{\{n_1\}}(\Omega) = \frac{1}{\sqrt{3}}(S_1(\Omega) + S_2(\Omega) + S_3(\Omega)), \quad (4.13a)$$

$$\mathcal{S}_{\{n_2\}}(\Omega) = \frac{1}{\sqrt{3}}(-S_1(\Omega) - S_2(\Omega) + S_3(\Omega)), \quad (4.13b)$$

$$\mathcal{S}_{\{n_3\}}(\Omega) = \frac{1}{\sqrt{3}}(S_1(\Omega) - S_2(\Omega) - S_3(\Omega)), \quad (4.13c)$$

$$\mathcal{S}_{\{n_4\}}(\Omega) = \frac{1}{\sqrt{3}}(-S_1(\Omega) + S_2(\Omega) - S_3(\Omega)). \quad (4.13d)$$

Here we use the short notations $S_k \equiv S_{(\ell=2, T_{2g}, k=1-3)}$ for real spherical harmonics Y_2^{1s} , Y_2^{1c} and Y_2^{2s} which belong to a three dimensional irreducible representation T_{2g} of O_h . (These spherical harmonics are proportional to the Cartesian components yz , zx and xy for $k = 1 - 3$.)

Below we consider the inter-site quadrupole interactions $V^{QQ}(\vec{n}, \vec{n}')$ which involve only the functions (4.13a-d). (There are also SAF's with $l = 4$ and 6 allowed by the $Pa\bar{3}$ symmetry³⁷ but those lead to weaker multipole interactions, Eq. (2.12).) We then rewrite Eq. (4.1) for a case when $\vec{n} \in \{n_1\}$ and $\vec{n}' \in \{n_{p'}\}$ ($p' = 2, 3, 4$):

$$\begin{aligned} \langle I_{fd} |_{\vec{n}} \langle I'_{fd} |_{\vec{n}'} V^{QQ}(\vec{n}, \vec{n}') | J'_{fd} \rangle_{\vec{n}'} | J_{fd} \rangle_{\vec{n}} = & - \sum_{\alpha\alpha'} \frac{\gamma^{\alpha\alpha'\alpha'}}{3} \\ & \times \{ c_{\{n_1\}}(i_\alpha j_\alpha) \delta(i_\beta j_\beta) \} \{ c_{\{n_{p'}\}}(i_{\alpha'} j_{\alpha'}) \delta(i_{\beta'} j_{\beta'}) \}, \end{aligned} \quad (4.14)$$

where, as before, $\alpha, \alpha', \beta, \beta'$ run over f and d , and where the same exclusion rules (if $\alpha = f$ then $\beta = d$ and vice versa) hold between α and β as well as between α' and β' . Here we have

$$\gamma^{\alpha\alpha'\alpha''} = \int dr r^2 \int dr' r'^2 \times \mathcal{R}_\alpha^2(r) \mathcal{R}_{\alpha'}^2(r') v_{\Lambda\Lambda}(\vec{n}, \vec{n}'; r, r'), \quad (4.15)$$

with $v_{\Lambda\Lambda}(\vec{n}, \vec{n}'; r, r')$ where $\vec{n} = (0, 0, 0)$, $\vec{n}' = (a/2)(0, 1, 1)$ and $\Lambda = (l = 2, T_{2g}, k = 1)$. The coefficients $c_{\{n_p\}}$ are defined as

$$c_{\{n_p\}}(i_\alpha j_\alpha) = \langle i_\alpha | \mathcal{S}_{\{n_p\}} | j_\alpha \rangle. \quad (4.16)$$

We introduce the quadrupolar density operators for the (fd) electron system on each sublattice:

$$\rho_{\alpha\alpha}^Q(\vec{n}_p) = \sum_{I,J} |I_{fd}\rangle c_{\{n_p\}}(i_\alpha j_\alpha) \delta_{i_\beta j_\beta} \langle J_{fd}|, \quad (4.17)$$

where $\vec{n}_p \in \{n_p\}$, $p = 1 - 4$. Here again $\alpha = \beta$, $\beta = d$ or $\alpha = d$, $\beta = f$. In terms of quadrupolar density operators, the quadrupolar interaction operator between two (fd) systems at site $\vec{n}_1 \in \{n_1\}$ and $\vec{n}_{p'} \in \{n_{p'}\}$ reads

$$V(\vec{n}_1, \vec{n}_{p'}) = - \sum_{\alpha\alpha'} \frac{\gamma^{\alpha\alpha'\alpha''}}{3} \rho_{\alpha\alpha}^Q(\vec{n}_1) \rho_{\alpha'\alpha''}^Q(\vec{n}_{p'}). \quad (4.18)$$

The mean-field potential at site \vec{n}_1 is obtained by summing $V(\vec{n}_1, \vec{n}_{p'})$ over the twelve nearest neighbors $\vec{n}_{p'}$ of \vec{n}_1 on the fcc lattice and by approximating the quadrupolar densities at these nearest neighbor sites by their thermal expectation values. The thermal expectation value of $\rho_{\alpha\alpha}^Q(\vec{n}_p)$ does not depend (*i.e.* is the same) on any site of a given sublattice and from the equivalence of the four sublattices it follows that it is the same on all sites of the fcc lattice. We then write

$$\langle \rho_{\alpha\alpha}^Q(\vec{n}_p) \rangle = \rho_{\alpha\alpha}^{Q,e}, \quad (4.19)$$

where the superscript e stand for thermal expectation. The mean-field potential is then given by

$$U^{MF}(\vec{n}_1) = -4 \sum_{\alpha\alpha'} \gamma^{\alpha\alpha'\alpha''} \rho_{\alpha\alpha}^Q(\vec{n}_1) \rho_{\alpha'\alpha''}^{Q,e}, \quad (4.20a)$$

or, explicitly,

$$U^{MF}(\vec{n}_1) = -(\lambda^{FF} \rho_F^{Q,e} + \lambda^{DF} \rho_D^{Q,e}) \rho_F^Q(\vec{n}_1) - (\lambda^{DD} \rho_D^{Q,e} + \lambda^{FD} \rho_F^{Q,e}) \rho_D^Q(\vec{n}_1), \quad (4.20b)$$

where we have defined $\lambda^{\alpha\alpha'\alpha''} = 4\gamma^{\alpha\alpha'\alpha''}$ and used F and D for $(\alpha\alpha)$, with $\alpha = f$ or d , respectively. The values of $\lambda^{\alpha\alpha'\alpha''}$ have been calculated before.¹⁸ Here we use the values $\lambda^{FF} = 2241$ K, $\lambda^{DF} = \lambda^{FD} = 6489$ K and $\lambda^{DD} = 18793$ K, calculated for α -Ce. Including the intra-site part $U|_{intra}$ and the crystal field $V_{CF}(\vec{n}_1)$, Eq. (4.1),

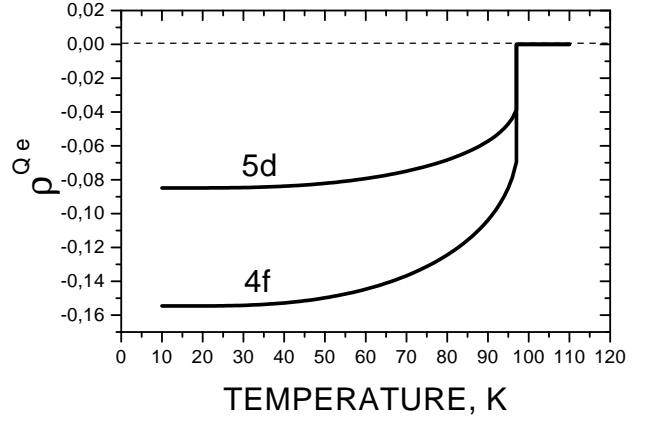


FIG. 1. Calculated evolution of the order parameter amplitudes $\rho_F^{Q,e}$ and $\rho_D^{Q,e}$ with temperature.

which are also present in the ordered phase, we obtain the full mean-field Hamiltonian

$$H^{MF}(\vec{n}_1) = U^{MF}(\vec{n}_1) + V_{CF}(\vec{n}_1) + U|_{intra}. \quad (4.21)$$

Finally, the expectation values (the order parameter amplitudes) $\rho_F^{Q,e}$ and $\rho_D^{Q,e}$, Eq. (4.19), are found by solving the following mean-field equations

$$\rho_F^{Q,e} = \frac{\text{Tr}\{\rho_F^Q(\vec{n}_1) \exp[-H^{MF}(\vec{n}_1)/T]\}}{\text{Tr}\{\exp[-H^{MF}(\vec{n}_1)/T]\}}, \quad (4.22a)$$

$$\rho_D^{Q,e} = \frac{\text{Tr}\{\rho_D^Q(\vec{n}_1) \exp[-H^{MF}(\vec{n}_1)/T]\}}{\text{Tr}\{\exp[-H^{MF}(\vec{n}_1)/T]\}}. \quad (4.22b)$$

It is convenient to rewrite these equations in the basis $|K_{fd}\rangle = |k_f k_d\rangle$ where H^{MF} is diagonal,

$$\rho_F^{Q,e} = \frac{1}{Z} \sum_{K_{fd}} c_{\{n_1\}}^F(k_f k_f) e^{-\epsilon_{K_{fd}}/T}, \quad (4.23a)$$

$$\rho_D^{Q,e} = \frac{1}{Z} \sum_{K_{fd}} c_{\{n_1\}}^D(k_d k_d) e^{-\epsilon_{K_{fd}}/T}, \quad (4.23b)$$

with

$$Z = \sum_{K_{fd}} e^{-\epsilon_{K_{fd}}/T}. \quad (4.23c)$$

Equations (4.20b)-(4.23c) are solved self-consistently. First, we introduce nonzero expectation values $\rho_F^{Q,e}$ and $\rho_D^{Q,e}$ in the mean-field Hamiltonian H^{MF} . After this we diagonalize H^{MF} and calculate new values of $\rho_F^{Q,e}$ and $\rho_D^{Q,e}$ at a given temperature T according to Eqs. (4.22a,b). Then we use these values to improve the mean-field Hamiltonian (4.21) and *etc.* until the input and output values of $\rho_F^{Q,e}$ and $\rho_D^{Q,e}$ converge. The results of the numerical calculation are shown in Fig. 1. The procedure outlined above converges very slowly in the vicinity of 100 K, *i.e.* at the phase transition point. We have

TABLE IV. Lowest levels of the energy spectrum of H^{MF} at $T = 0$ and magnetic moments \mathcal{M}_z for α -Ce. Numbers in parentheses stand for degeneracy; the site group is $S_6 = C_3 \times i$.

Γ, μ	ϵ_i , in K	$(\epsilon_i - \epsilon_1)$, in K	\mathcal{M}_z , in μ_B
$E, 1$ (2)	-10888.5	0.0	± 2.0683
$A, 1$ (1)	-10721.4	167.1	0
$A, 2$ (1)	-10699.7	188.8	0
$E, 2$ (2)	-10542.2	346.3	± 1.0116
$E, 3$ (2)	-10427.1	461.4	± 0.4882

found the transition temperature $T_1 = 97$ K and the order parameter discontinuities $\rho_F^{Qe}(T_1) = -0.06956$ and $\rho_D^{Qe}(T_1) = -0.03875$. (From symmetry considerations it follows that the phase transition is of first order.¹⁷) At $T = 0$ the averages in Eq. (4.19) are taken over the ground state doublet and we obtain $\rho_F^{Qe}(T = 0) = -0.15462$, $\rho_D^{Qe}(T = 0) = -0.08485$. The lowest five levels of H^{MF} for this case are given in Table IV. Notice, however, that unlike the crystal field V_{CF} the mean field potential U^{MF} , Eq. (4.20b), and the Hamiltonian H^{MF} depend implicitly on temperature T since the order parameter amplitudes ρ_F^{Qe} and ρ_D^{Qe} change with temperature, Fig. 1, and the energy splittings $(\epsilon_i - \epsilon_1)$ decrease with increasing T up to T_1 . Above the phase transition point the spectrum transforms discontinuously to that of γ -Ce, Table III. The double degenerate states (the representations E in Table IV) are due to time-reversal symmetry.³⁶ For a further discussion of the energy spectrum of H^{MF} we refer to Appendix A, where we study the magnetic moments of the two electrons.

V. DISCUSSION AND CONCLUSIONS

This work is an extension of our previous model of the $\gamma - \alpha$ phase transition in Ce based on the idea of quadrupole ordering.^{17,18} In addition to the inter-site quadrupolar couplings here we consider the multipolar intra-site (direct Coulomb and exchange) interactions between one localized $4f$ electron and one delocalized $5d$ electron taken instantaneously at a same cerium site. The intra-site interactions are treated exactly in the adopted $4f5d$ model. In γ -Ce we have calculated and analyzed the crystal electric field excitations, Table III. In α -Ce the $Pa\bar{3}$ quadrupolar ordering sets in and drives the $\gamma - \alpha$ phase transition. The quadrupolar order has been studied in the mean-field approximation, Eqs from (4.20b) to (4.23c). We have calculated the phase transition temperature ($T_1 = 97$ K) and the evolution of the order parameter amplitudes (ρ_F^{Qe} and ρ_D^{Qe} , see Fig. 1) by solving self-consistently the mean-field equations (4.20b)-(4.23c). We have shown before^{17,18} that quadrupolar ordering in the $Pa\bar{3}$ structure leads to a uniform lattice contraction conserving the cubic symmetry of the lattice.

The change of the energy spectrum at the transition implies a change of the magnetic susceptibility. Indeed, we have found that the calculated magnetic moments are different in γ - and α -Ce. Moreover, in the ground state of α -Ce the magnetic moment of the $4f$ electron is bound to the magnetic moment of the $5d$ electron (a qualitative origin of this correlation is given in Appendix B). The lowest magnetic excited state ($E, 2$ in Table IV) is separated from the ground state by an energy gap $\Delta\epsilon \sim 350$ K which is much larger than a typical crystal field excitation in the γ phase, Table III. However, here our treatment is incomplete. Although the present model carefully takes into account the intra-site interactions it does not describe properly the metallic bonding in Ce.

The question of correspondence between our approach and electron band structure calculations deserves a special attention. As we have discussed in Sec. II, in the ‘‘muffin-tin’’ approximation a localized $4f$ electron experiences only a field of spherical symmetry and occupies a 14-fold degenerate level. The localized states of the $4f$ electron then are uncorrelated with the states of conduction electrons, because the spherical component of the $4f$ density is independent of its spin (s_z) and orbital (m_f) projections. In our study we show that this simple picture is not correct and there exist strong local correlations between localized $4f$ and delocalized $5d$ electrons omitted in a conventional band structure calculation. These correlations arise due to the Coulomb on-site repulsion and reflect the electronic term structure of atomic cerium, Sec. III. We show that the excitations of the $4f$ electron are combined with those of $5d$ electron in a single spectrum, which is sensitive to crystal site symmetry because of intersite interactions, Sec. IV.

In principle, band structure calculations with the full potential (FP) extension (so-called FP-linear muffin-tin (FLMTO)²⁵ and FP-linear augmented plane wave (FLAPW)²³ methods) are capable of dealing with non-spherical contributions of density and potential. Provided that the site symmetry is introduced explicitly, calculations with the full potential option can describe some, but not all structural properties associated with the $Fm\bar{3}m \rightarrow Pa\bar{3}$ transformation. The reason is that the band structure calculations are based on the single-determinant Hartree-Fock method. In our treatment each local two-electron basis function, Eqs. (2.2)-(2.6), corresponds to a Slater determinant (with the permutation property (2.7)). The solutions are expressed as linear combinations of all these functions (determinants). As such, our method corresponds to a many determinant treatment or configurational interaction (CI). Clearly, it is not the case with the band structure approach. This explains why the conventional band structure treatment is missing some intra- and inter-site correlations which are taken into account in our approach.

The other drawback of the FP electronic band structure calculations is connected with the local density approximation (LDA). In the LDA the exchange potential

is a function of density and has the full (unit) symmetry of the crystal. This implies that the density and the LDA exchange potential are invariant under inversion in both phases. Expanding the exchange potential in terms of spherical harmonics on a cerium site we find that only harmonics with even l are allowed by the inversion symmetry, i.e., $l = 2, 4$ etc. However, as we observe from Eq. (3.10b) the contributions with *odd* values of l are relevant for the exchange between $4f$ and $5d$ electrons, namely $l = 1, 3$ and 5 . Thus, these terms are washed away by the LDA treatment.

On the other hand, the present method should be extended to include the metallic bonding in Ce explicitly. In our opinion, a combination of the local correlations with the band structure approach constitutes a challenge for further studies. We are presently working on the problem and hope to achieve this by employing the valence bond (VB) or Heitler-London approach. The VB method is more difficult to implement, but usually it gives a better description of chemical bonding than the method of molecular orbitals.^{36,43} The alternative approach is a merger with one of the existing band structure methods and introducing in some way a CI treatment.

Finally, we would like to mention again that we are aware of the fact that our approach is not complete, but it certainly underlines the importance of the structural factors and the local correlations for this long-standing problem. We have shown that the local electronic interactions can trigger the $\gamma \rightarrow \alpha$ phase transition in Ce, but other aspects of the problem (in particular, chemical bonding etc.) should also be taken into account. As before,^{17,18} we suggest synchrotron radiation experiments in order to check the appearance of weak superstructure reflections in the $Pa\bar{3}$ structure (α -Ce) and to study diffuse scattering in γ - and α -Ce.

The present model generalizes our initial approach, Ref. 17, for a many electron case. The method can be applied (as it has been done for TmTe in Ref. 26) to study quadrupole orderings¹⁵ in lanthanides and their compounds (DyB₂C₂,²⁷ DyB₆,²⁸ UCu₂Sn,²⁹ PrPb₃,³⁰ YbAs,³¹ YbSb³²) where a few f electrons at each site are involved in the process of ordering.

ACKNOWLEDGMENTS

We thank D.V. Lopaev for references on atomic spectra. This work has been financially supported by the Fonds voor Wetenschappelijk Onderzoek, Vlaanderen.

APPENDIX A:

In order to calculate the effective magnetic moments and the Lande g -factors we study the polarization of electronic states in a small external magnetic field H . In such case we add to the Hamiltonian \mathcal{H} (that is $U|_{intra}$, Eq.

(3.16), for the atomic case, $U|_{intra} + V_{CEF}$, Eq. (4.11), for γ -Ce, and $U|_{intra} + V_{CEF} + U^{MF}$, Eq. (4.21), for α -Ce) a magnetic term

$$V_{mag} = -\mathcal{M}_z \cdot H. \quad (\text{A1a})$$

Here

$$\mathcal{M}_z = (\mathcal{M}_z(f) + \mathcal{M}_z(d)), \quad (\text{A1b})$$

with

$$\vec{\mathcal{M}}(f) = \mu_B(\vec{L}(f) + 2\vec{S}(f)), \quad (\text{A2a})$$

$$\vec{\mathcal{M}}(d) = \mu_B(\vec{L}(d) + 2\vec{S}(d)), \quad (\text{A2b})$$

μ_B being the Bohr magneton. The matrix elements of V_{mag} read

$$\begin{aligned} \langle I_{fd} | V_{mag} | J_{fd} \rangle = & (\langle i_f | \mathcal{M}_z(f) | j_f \rangle \delta_{i_d j_d} \\ & + \langle i_d | \mathcal{M}_z(d) | j_d \rangle \delta_{i_f j_f}) \cdot H, \end{aligned} \quad (\text{A3})$$

where $\langle i_f | \mathcal{M}_z(f) | j_f \rangle$ and $\langle i_d | \mathcal{M}_z(d) | j_d \rangle$ are one-particle matrix elements which can be easily computed. If we diagonalize the matrix of $(\mathcal{H} + V_{mag})$, then the degeneracies of the energy terms are lifted and the magnetic moment of each sublevel ν is given by

$$\mathcal{M}_z(\epsilon_\nu) = \langle \epsilon_\nu | \mathcal{M}_z | \epsilon_\nu \rangle, \quad (\text{A4})$$

where $\{\epsilon_\nu\}$ stands for the energy levels $\{E_{fd}\}$ or $\{\epsilon_i\}$ given in Tables II or III and IV, for the atomic case (intra-site), the γ -phase and the α -phase, respectively. The results for \mathcal{M}_z for the solid state phases are quoted in Tables III and IV. The Lande g -factors are obtained from

$$\mathcal{M}_z(\epsilon_\nu, j) = \mu_B g(\epsilon_\nu) j, \quad (\text{A5})$$

where j is the z -projection of a total angular momentum: $j = -J, -J + 1, \dots, +J$. The calculated g -factors for the atomic case, Table II, are close to the experimental values.³⁴

In case of γ -Ce and α -Ce the z -axis is the [001] axis of the cubic crystal. For γ -Ce only triply degenerate levels of T_1 or T_2 symmetry have nonzero magnetic moments which are $-\mathcal{M}(t)$, 0 and $+\mathcal{M}(t)$, where $\mathcal{M}(t) > 0$ and $t = (T_1, \mu)$ or $t = (T_2, \mu)$, Table III. For α -Ce only double degenerate levels of E symmetry have nonzero magnetic moments which are $-\mathcal{M}(e)$ and $+\mathcal{M}(e)$, where $\mathcal{M}(e) > 0$ and $e = (E, \mu)$, Table IV. The double degenerate states are due to time-reversal symmetry.³⁶ It is worth noting that in the ground state ($E, 1$) the magnetic moment of the localized $4f$ electron is not independent. It is attached to the magnetic moment of the $5d$ conduction electron. The change of sign of the magnetic moment of the $5d$ electron under the time reversal symmetry now requires the concomitant change of the sign of the magnetic moment of the localized $4f$ electron. We discuss the origin of this correlation in Appendix B. Since the $5d$ electron belongs to the conduction band, the ground

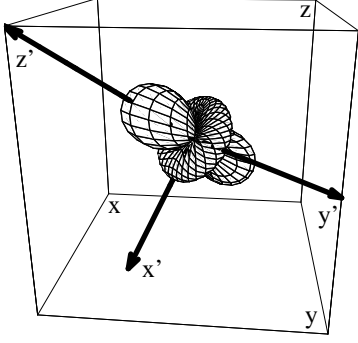


FIG. 2. The transformation $\{x, y, z\} \rightarrow \{x', y', z'\}$ (the Euler angles are $\alpha = \pi/4$, $\beta = \arccos(1/\sqrt{3})$, $\gamma = 0$ for passive and (γ, β, α) for active rotations), and the function $\mathcal{S}_{\{n_1\}}$, Eq. (4.13a).

state $(E,1)$ gives rise to a Pauli paramagnetism. The other levels given in Table IV represent excited states of α -Ce. However, we observe that the first (representation $A,1$ of Table IV) and the second state $(A,2)$ are nonmagnetic. The first magnetic excited state $(E,2)$ is separated from the ground state by an energy gap of $\Delta\epsilon \sim 350$ K. This observation could explain the absence of the Curie-Weiss contribution to the magnetic susceptibility χ_α at temperatures $T < T_1$.

APPENDIX B:

We consider the function $\mathcal{S}_{\{n_1\}}(\Omega)$, Eq. (4.13a), in a new coordinate system of axes $\{x', y', z'\}$ where the z' -axis corresponds to the cubic $[111]$ -axis, Fig. 2. Then

$$\mathcal{S}_{\{n_1\}}(\Omega) = Y_{l=2}^{m=0}(\Omega'), \quad (\text{B1})$$

where Ω' stands for the polar angles (Θ', ϕ') in the new system of axes. The coefficients $c_{\{n_1\}}^F(i_f j_f)$ and $c_{\{n_1\}}^D(i_d j_d)$, Eq. (4.16), become diagonal in the new basis,

$$c_{\{n_1\}}(i_\alpha j_\alpha) = \langle i_\alpha | Y_2^0 | i_\alpha \rangle \delta_{i_\alpha j_\alpha}, \quad (\text{B2})$$

that facilitates the calculation of the mean-field interaction $U^{MF}(\vec{n}_1)$, Eq. (4.20b). In this Appendix we show that U^{MF} is minimized for the following two functions

$$\mathcal{Y}_{L=5}^{M_L=5} = Y_3^3(\Omega'_f) \cdot Y_2^2(\Omega'_d), \quad (\text{B3a})$$

$$\mathcal{Y}_{L=5}^{M_L=-5} = Y_3^{-3}(\Omega'_f) \cdot Y_2^{-2}(\Omega'_d), \quad (\text{B3b})$$

where Ω'_f and Ω'_d refer to the polar coordinates of $4f$ and $5d$ electron, respectively.

Indeed, there are 11 functions $\mathcal{Y}_{L=5}^{M_L}$ ($M_L = -5, -4, \dots, 5$), which form a basis of the two-particle irreducible representation H of the group $SO(3)$ of three dimensional rotations. (In Eq. (B3) we quote only two functions, the others can be obtained from the Table

4³ of Ref. 22.) In the LS (Russel-Saunders) coupling the triplet 3H lies lower in energy than the singlet 1H , Table I. If now we include the diagonal mean-field coupling U^{MF} , we obtain that the six states with the orbital components \mathcal{Y}_5^5 and \mathcal{Y}_5^{-5} and with the spin components $M_S = -1, 0, 1$ (originating from the 3H triplet) go down in energy. These six states are further split by the spin-orbit coupling in three magnetic doublets of E symmetry of the site group $S_6 = C_3 \times i$. Finally, in the full treatment (Sect. 4.2) the middle doublet is split by the crystal field in two nonmagnetic components of A symmetry. This explains qualitatively the origin of the four lowest levels of the $Pa\bar{3}$ structure of α -Ce, Table IV. The real situation is more complex since there is a mixing of different configurations in atomic cerium. Nevertheless, a considerable admixture of 3H configuration (29%) is found in the ground state of atomic cerium³⁴ and it is very likely to occur in γ -Ce.

In α -Ce orbital functions of $5d$ electrons on neighboring sites overlap giving rise to band structure effects. Here we consider these effects only as a perturbation to the ground state $E, 1$, Table IV. Then in tight-binding approximation a band state with the wave vector \vec{k} is a mixture of the d -functions $Y_2^2(\Omega'_d)$ and $Y_2^{-2}(\Omega'_d)$. However, as we have seen earlier, these electronic $5d$ states are bound to the two $4f$ electron states $Y_3^3(\Omega'_f)$ and $Y_3^{-3}(\Omega'_f)$ and form the two-electron functions $\mathcal{Y}_{L=5}^{M_L=5}$ and $\mathcal{Y}_{L=5}^{M_L=-5}$, Eqs. (B3a,b). Therefore, the resulting doubly degenerate states are in fact two-electron band states with the energy $\mathcal{E}_+(\vec{k}) = \mathcal{E}_-(\vec{k})$ (the sign $+$ or $-$ here stands for the two-electron time reversed band states). In the magnetic field these two bands become split, $\mathcal{E}_+(\vec{k}) \neq \mathcal{E}_-(\vec{k})$, and this leads to a temperature independent Pauli paramagnetism.

¹ D. C. Koskenmaki and K. A. Gschneidner, Jr., *Handbook on the Physics and Chemistry of Rare Earths*, ed. K. A. Gschneidner, Jr., and L. Eyring (Amsterdam: North-Holland, 1978), p. 337.

² M.I. McMahon and R.J. Nelves, Phys. Rev. Lett. **78**, 3884 (1997).

³ D. Malterre, M. Gironi, Y. Baer, Adv. Phys. **45**, 299 (1996).

⁴ B. Johansson, Phil. Mag. **30**, 469 (1974).

⁵ B. Johansson, I.A. Abrikosov, M. Alden, A.V. Ruban, H.L. Skriver, Phys. Rev. Lett. **74**, 2335 (1995).

⁶ Z. Szotek, W.M. Temmerman and H. Winter, Phys. Rev. Lett. **72**, 1244 (1994); A. Svane, Phys. Rev. Lett. **72**, 1248 (1994); A. Svane, Phys. Rev. B **53**, 4275 (1996).

⁷ T. Jarlborg, E. G. Moroni, and G. Grimvall, Phys. Rev. B **55**, 1288 (1997).

⁸ J. Lægsgaard and A. Svane, Phys. Rev. B **59**, 3450 (1999).

- ⁹ J. W. Allen, R. M. Martin, Phys. Rev. Lett. **49**, 1106 (1982); J. W. Allen, L. Z. Liu, Phys. Rev. B **46**, 5047 (1992).
- ¹⁰ M. Lavagna, C. Lacroix, M. Cyrot, Phys. Lett. **90A**, 710 (1982); J. Phys. F **13**, 1007 (1985).
- ¹¹ O. Gunnarsson, K. Schönhammer, Phys. Rev. Lett. **50**, 604 (1983); O. Gunnarsson, K. Schönhammer, Phys. Rev. B **28**, 4315 (1983).
- ¹² N. E. Bickers, D. L. Cox, J. W. Wilkins, Phys. Rev. B **36**, 2036 (1987).
- ¹³ M.B. Zöflf, I.A. Nekrasov, Th. Pruschke, V.I. Anisimov, and J. Keller, Phys. Rev. Lett. **87**, 276403 (2001); K. Held, A.K. McMahan, and R.T. Scalettar, Phys. Rev. Lett. **87**, 276404 (2001).
- ¹⁴ S. Endo, H. Sasaki and T. Mitsui, J. Phys. Soc. Jap. **42**, 882 (1977).
- ¹⁵ P. Morin and D. Schmitt, in *Ferromagnetic Materials*, K.H.J. Buschow and E.P. Wohlfarth Eds. (North-Holland, Amsterdam, 1990), v. 5, p. 1.
- ¹⁶ G. Eliashberg and H. Capellmann, JETP Lett. **67**, 125 (1998).
- ¹⁷ A.V. Nikolaev and K.H. Michel, Eur. Phys. J. B **9**, 619 (1999); *ibid.* **17**, 363 (2000).
- ¹⁸ A.V. Nikolaev and K.H. Michel, Eur. Phys. J. B **17**, 15 (2000).
- ¹⁹ J.W. van der Eb, A.B. Kuz'menko, and D. van der Marel, Phys. Rev. Lett. **86**, 3407 (2001).
- ²⁰ K.H. Michel, J.R.D. Copley, D.A. Neumann, Phys. Rev. Lett. **68**, 2929 (1992); K.H. Michel, Z. Phys. B Cond. Matter **88**, 71 (1992).
- ²¹ W.I.F. David, R.M. Ibberson, T.J.S. Dennis, J.P. Hare, and K. Prassides, Europhys. Lett. **18**, 219 (1992); P.A. Heiney, G.B.M. Vaughan, J.E. Fischer, N. Coustel, D.E. Cox, J.R.D. Copley, D.A. Neumann, W.A. Kamitakahara, K.M. Creegan, D.M. Cox, J.P. McCauley, Jr., A.B. Smith III, Phys. Rev. B **45**, 4544 (1992).
- ²² E.U. Condon and G.H. Shortley, *The theory of atomic spectra*, (University Press, Cambridge, 1967).
- ²³ D.D. Koelling and G.O. Arbman, J. Phys. F **5**, 2041 (1975); D.J. Singh, *Planewaves, Pseudopotentials and the LAPW method*, (Kluwer, Boston, 1994).
- ²⁴ O.K. Andersen, Phys. Rev. B **12**, 3060 (1975); H.L. Skriver, *The LMTO Method*, (Springer-Verlag, Berlin, 1984).
- ²⁵ P. Söderlind, O. Eriksson, B. Johansson, and J.M. Wills, Phys. Rev. B **50**, 7291 (1994); J.M. Wills and O. Eriksson, Phys. Rev. B **45**, 13879 (1992).
- ²⁶ A.V Nikolaev and K.H. Michel, Phys. Rev. B **63**, 104105 (2001).
- ²⁷ H. Yamauchi, H. Onodera, K. Ohoyama, T. Onimaru, M. Kosaka, M. Ohashi and Y. Yamaguchi, J. Phys. Soc. Jpn. **68**, 2057 (1999); K. Indoh, H. Onodera, H. Yamauchi, H. Kobayashi and Y. Yamaguchi, J. Phys. Soc. Jpn. **69**, 1978 (2000); K. Hirota, N. Oumi, T. Matsumura, H. Nakao, Y. Wakabayashi, Y. Murakami, Y. Endoh, Phys. Rev. Lett. **84**, 2706 (2000). Y. Tanaka, T. Inami, T. Nakamura, H. Yamauchi, H. Onodera, K. Ohoyama and Y. Yamaguchi, J. Phys. Condens. Matter **11**, L505 (1999).
- ²⁸ H. Onodera, K. Indoh, H. Kobayashi, S. Kunii and Y. Yamaguchi, J. Phys. Soc. Jpn. **69**, 1100 (2000).
- ²⁹ T. Suzuki, I. Ishii, N. Okuda, K. Katoh, T. Takabatake, and T. Fujita, Phys. Rev. B **62**, 49 (2000).
- ³⁰ T. Tayama, T. Sakakibara, K. Kitami, M. Yokoyama, K. Tenya, H. Amitsuka, D. Aoki, Y. Onuki, Z. Kletowski, J. Phys. Soc. Jpn. **70**, 248 (2001).
- ³¹ L. Keller, W. Henggeler and A. Furrer, Europhys. Lett. **26**, 353 (1994); P.J. von Ranke, A.L. Lima, E.P. Nobrega, X.A. de Silva, A.P. Guimaraes, and I.S. Oliveira, Phys. Rev. B **63**, 024422 (2000).
- ³² K. Hashi, H. Kitazawa, A. Oyamada, and H.A. Katori, J. Phys. Soc. Jpn. **70**, 259 (2001).
- ³³ D. Glötzel, J. Phys. F **8**, L163 (1978); W.E. Pickett, A.J. Freeman, and D.D. Koelling, Phys. Rev. B **23**, 1266 (1981).
- ³⁴ W.C. Martin, R. Zalubas, and L. Hagan, *Atomic Energy Levels - The Rare-Earth Elements*, Natl. Stand. Ref. Data Ser., Natl. Bur. Stand. (U.S.) **60** (1978) and original references therein; NIST Atomic Spectra Database (http://physics.nist.gov/cgi-bin/AtData/main_asd).
- ³⁵ W. Heitler and F. London, Z. Physik **44**, 455 (1927);
- ³⁶ M. Tinkham, *Group Theory and Quantum Mechanics*, (McGraw-Hill, New York, 1964).
- ³⁷ C.J. Bradley and A.P. Cracknell, *The Mathematical Theory of Symmetry in Solids*, (Clarendon, Oxford, 1972).
- ³⁸ H. Yasuda and T. Yamamoto, Prog. Theor. Phys. **45**, 1458 (1971); R. Heid, Phys. Rev. B **47**, 15912 (1993).
- ³⁹ The expressions (4.7) and (4.10a) hold even if the summation is taken beyond nearest neighbors: A.V. Nikolaev and P.N. Dyachkov, Int. J. Quantum Chem. (2002), in press, cond-mat/0203015.
- ⁴⁰ G.V. Ionova and A.V. Nikolaev, Phys. Stat. Sol. (b) **162**, 451 (1990).
- ⁴¹ The values of B_4^d , B_4^f and B_6^f were calculated taking into account all neighbors, see Ref. 39.
- ⁴² K.R. Lea, M.J.M. Leask, and W.P. Wolf, J. Phys. Chem. Solids **23**, 1381 (1962).
- ⁴³ S. Wilson, *Electron correlation in molecules*, (Clarendon Press, Oxford, 1984), p. 227.